Applied Physics Express 5 (2012) 016602
DOI: 10.1143/APEX.5.016602

Microwave Atomic Force Microscopy: Quantitative Measurement and Characterization of Electrical Properties on the Nanometer Scale

Lan Zhang, Yang Ju*, Atsushi Hosoi, and Akifumi Fujimoto

Department of Mechanical Science and Engineering, Nagoya University, Nagoya 464-8603, Japan

Received September 22, 2011; accepted December 1, 2011; published online December 21, 2011

In this paper, we report a noncontact and quantitative method of evaluating and characterizing electrical properties with a nanometer-scale spatial resolution. Microwave atomic force microscopy (M-AFM) can be used to obtain the topography and microwave image of materials in one scanning process simultaneously. Under the frequency modulation (FM) AFM mode, we successfully applied M-AFM to create a microwave image of a Au nanowire with a spatial resolution of 170 nm. Moreover, based on the analytical and explicit expressions proposed, M-AFM can implement the quantitative evaluation and characterization of the local conductivity of materials on the nanometer scale.

Atomic force microscopy (AFM)[1,2] has played an important role in nanoscale science and technology. Recently, several attempts based on atomic force microscopy have been made to characterize the electrical information of materials on the nanometer scale, such as conducting atomic force microscopy (C-AFM),[3] scanning capacitance microscopy (SCM),[4] and electrostatic force microscopy (EFM).[5] Although C-AFM can be used for the nanoscale electrical characterization of thin films, it is only suitable for measuring conducting materials, and the contact between the scanning AFM tip and the sample surface may cause scratch damage to the sample. SCM can be used to characterize electrical properties by measuring the capacitance between the tip of the probe and the sample. However, it suffers from a limited spatial resolution and is sensitive to the thickness of the specimen. EFM, including Kelvin probe force microscopy (KFM),[6] scanning surface potential microscopy (SSPM),[7] and scanning Maxwell-stress microscopy (SMM),[8] can be used to measure the surface electrical potential of materials by detecting the electrostatic force between the probe tip and the sample. However, the results are affected by the sample surface chemistry and atmospheric conditions, since the van der Waals forces and chemical bonding forces cannot be excluded during the measurement.

On the other hand, microwave measurements have been of great interest to many researchers because microwaves can propagate easily in air, and the sample response is directly related to the electrical properties of the material.[9] A variety of microwave methods with well-calibrated instruments have been developed to obtain the microscopic electrical information.[10–16] However, to evaluate the electrical properties of materials using microwaves, it is necessary to keep the standoff distance between the microwave probe and the sample constant because microwave signals in the near-field are extremely sensitive to this distance.

Recently, we proposed a novel microwave atomic force microscopy (M-AFM).[17–21] By combining the advantages of AFM with microwave-based measurement, M-AFM has the ability to sense the topography and microwave image simultaneously with a high spatial resolution. Although the possibility of evaluating the conductivities of metallic materials has been quantitatively demonstrated,[21] the measurement of the distribution of the conductivities and the quantitative evaluation of the conductivities from microwave images have not been realized yet. Thus, in this work, the quantitative measurement of the local conductivity of samples is realized by applying a newly proposed analytical and explicit evaluation equation.

An undoped GaAs wafer was used as the substrate of the M-AFM probe to restrict the attenuation of microwaves in it. To obtain the desired structure, wet etching was used to fabricate the M-AFM probe.[18] To make the microwave signals propagate well in the probe, two Au films were deposited on the top and bottom surfaces of the probe by electron beam (EB) evaporation to form a parallel-plate waveguide. Both plane surfaces of the probe, which are evaporated Au films, are connected at the end of the probe cantilever. However, there is no Au film on the sides of the M-AFM probe. Finally, a nanoslit at the tip of the probe was fabricated by a focused ion beam (FIB) process, from which the microwave emits.

Figure 1(a) shows schematically the integrated measurement system of M-AFM. In our M-AFM system, the initial microwave signals working at a frequency of 16.66 GHz are generated with a microwave generator. Then, the frequency of the microwave signal is extended by a six-time frequency multiplier, resulting in a stable operational frequency of 94 GHz. The microwave signal transmits through an isolator and a circulator and propagates into the M-AFM probe. The M-AFM probe consists of a homogeneous parallel plate and a nanoslit that cuts across the tip apex. These special structures allow microwave signals to propagate through the probe and emit from the tip of the M-AFM probe. When the M-AFM probe is located above a sample surface, the nanoslit on the tip acts as a transmitter of microwave signals emitted onto the surface of the sample and as a receiver of the microwave signals reflected from the measured sample. Finally, a detector connected to the circulator measures the microwave signals received by the tip of the probe and indicates the voltage converted from the reflected microwave signals. The measured signals are synchronized with the position information obtained from the AFM scanner to create the microwave image. Figure 1(b) shows the measured width and height of a single Au nanowire on a glass substrate to be 480 and 210 nm, respectively, as obtained with M-AFM. The Au nanowires were formed by partially etching the Au film using FIB with a width of 500 nm and a space of 400 nm, where the Au film was coated on a glass-wafer substrate of 200 nm thickness by EB evaporation. Figure 1(c) shows the

*E-mail address: ju@mech.nagoya-u.ac.jp

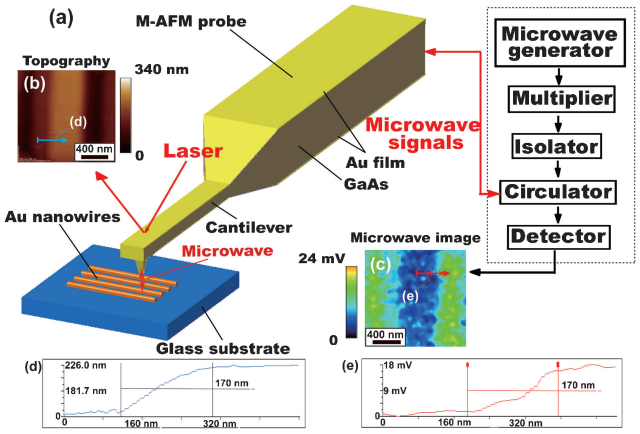

Fig. 1. Microwave atomic force microscopy setup and typical surface topography and microwave image of a nanowire sample: (a) schematic graph of the AFM compact microwave instrument setup and schematic diagram of the Au nanowires scanned using the M-AFM probe; (b) topography image of measured sample; (c) microwave image of the nanowire created from the voltage of the measured microwave signals; (d) crossing profile corresponding to the arrow in the topography image; (e) crossing profile of the selected area in the microwave image.

microwave image of the Au nanowire, where the voltage was measured from the reflected microwave signal without calibration. The M-AFM worked in frequency modulation (FM) mode (noncontact mode). The measurements were performed in air ambient, with a working environment temperature of 26.0 °C and a relative humidity of 50%. The scanning area and scanning speed were $1.5 \times 1.5\,\mu m^2$ and 500 nm/s, respectively. In Fig. 1(e), it is noted that the difference in the measured voltages of the Au and glass substrate is approximately 16 mV, and the spatial resolution is 170 nm. This result illustrates that M-AFM is capable of sensing the microwave image of a nanostructure. In contrast to the traditional four-point method, which requires some nanowires to be in suitable positions for conductivity measurements by dispersing the nanowires onto an insulated substrate with electrode arrays, M-AFM can spot the nanostructures directly and measure the microwave image and topography simultaneously.

For quantitative measurement, the operating frequency of M-AFM is set at 94 GHz. The high-frequency microwaves are easy to propagate in the waveguide and emit from the nanoslit on the probe tip. Since the width of the nanoslit is around 100 nm, the field of microwave interacting with the measured materials can be considered to be in the 100 nm order. Thus, if the thickness of the measured materials is larger than 100 nm, the reflection from the bottom surface of the sample can be neglected. Therefore, only the reflection from the top surface needs to be considered. Moreover, the diode detector works in a small signal range, where it is considered to be a square-law detector.[22] Therefore, while keeping the standoff distance between the tip of the M-AFM probe and samples constant, the output reflected voltage V, which varies only with the conductivity of the sample, has a relationship with the squared absolute value of the top surface reflection coefficient $|\Gamma_s|^2$ as

$$V = k_0|\Gamma_s|^2 + b_0. \quad (1)$$

The two undetermined constants k_0 and b_0 can be calibrated with two samples whose conductivities are known.

For good conductors, which are used in this experiment, the surface reflection coefficient[23] $|\Gamma_s|$ can be written as[24]

$$|\Gamma_s| = \left|\frac{1-\sqrt{\sigma/j\omega\varepsilon_0}}{1+\sqrt{\sigma/j\omega\varepsilon_0}}\right|, \quad (2)$$

where ε_0 and σ represent the permittivity of free space and the conductivity of the measured material, respectively, and ω is the angular frequency of the microwave. For semiconductor or isolating materials, similar equations can also be constructed.[9,24] Then, the conductivity can be determined from eq. (2) as

$$\sigma = \omega\varepsilon_0 \frac{4|\Gamma_s|^2 - (|\Gamma_s|^2+1)^2}{(|\Gamma_s|^2+1)\sqrt{4|\Gamma_s|^2 - (|\Gamma_s|^2-1)^2} - 4|\Gamma_s|^2}. \quad (3)$$

After k_0 and b_0 in eq. (1) are calibrated using two reference samples with known conductivities, the conductivities of any sample can be calculated from the measured voltage.

It should be noted that eqs. (2) and (3) are derived under the plane wave condition, while the probe works in near-field mode. Although near-field analysis may further improve the precision of evaluation results, it requires more reference samples, which will increase the complexity of the measurement. Since the tested material was very close to the open end of the probe tip (the standoff distance of several nanometers was extremely small as compared with the waveguide width (~100 nm) and the wavelength), this problem can be equivalent to the case that the material surface is terminated at the end of the waveguide, which can be represented by the plane wave model. Therefore, the plane wave approximation is used in this work.

Five different metallic films (Cu, Pb, Al, Co, and Zn) were prepared by EB evaporation method for the quantitative measurement. The tested electrical conductivities by the four point probe van der Pauw method were obtained as the standard values for calibration and evaluation of M-AFM results. The tested electrical conductivities of these metal films are in the range of 4.46×10^6 to 5.68×10^7 S/m. The scanning area was $2 \times 2\,\mu m^2$, and the scanning speed was 1 μm/s. Before scanning, we set the original voltage to be zero while maintaining a constant distance of 2.6 μm between the probe tip and the sample. During the scanning process, the standoff distance between the probe tip and samples was fixed at several nanometers using the atomic force, and the voltage corresponding to the inspected sample was measured. Figures 2(a)–2(e) show the topographies and microwave images of the five samples. The variations of the measured voltages for the five samples are less than ±0.46 mV, which is much smaller than the dynamic range of the M-AFM. The signal-to-noise ratio of the M-AFM measurements was evaluated to be 20.14 dB on average. The Fig. 2(f) shows the variation margins of measured local voltages for samples with different conductivities. Using the measured voltages of two samples obtained from Figs. 2(a) and 2(b) (4.89 mV for Cu and 18.01 mV for Pb on average) and their tested conductivities (5.68×10^7 S/m for Cu and 4.46×10^6 S/m for Pb) for calibration, the two undetermined constants in eq. (1) were calculated to be $k_0 = -5.9632$ and $b_0 = 5.9629$. Then, the conductivities of Al, Co, and Zn samples were evaluated with

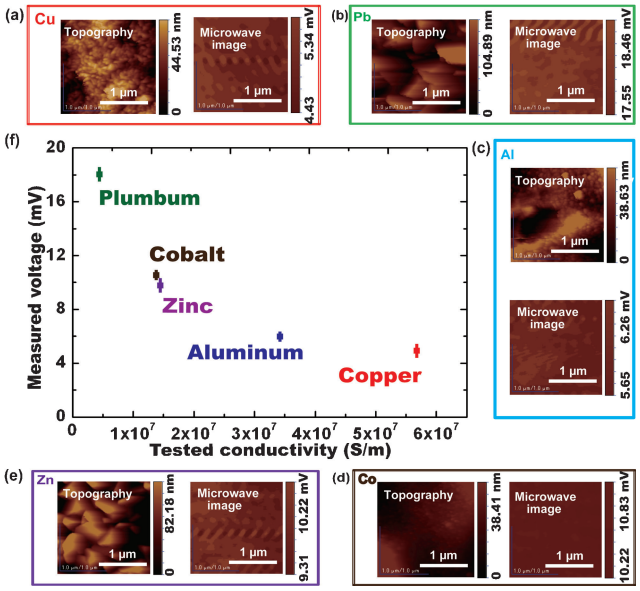

Fig. 2. (a)–(e) Clockwise from the top-left corner, topographies and M-AFM images of Cu, Pb, Al, Co, and Zn samples; (f) variation margins of measured local voltages for samples with different conductivities.

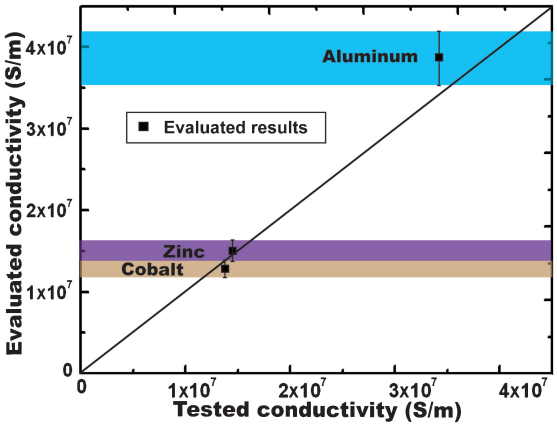

Fig. 3. Evaluated conductivities of the samples in comparison with tested conductivities of them.

eqs. (1) and (3) by using the measured voltages obtained from Figs. 2(c)–2(e). Figure 3 shows the evaluated results versus the tested values of Al, Co, and Zn samples.

It is noted from Figs. 2(a)–2(e) that no correlation can be observed between the microwave images and their corresponding geometry images. In other words, the variations of the measured local voltages are not caused by the surface morphology. The main causes of error bars of the evaluated conductivities are as follows. Firstly, the film samples prepared by EB evaporation were not homogenous in the microscopic view, and the distribution of conductivity was location dependent (local conductivity). It is believed that the variation margins of measured local voltages [see Fig. 2(f)] by M-AFM caused the error bars of the evaluated conductivities. Secondly, the microwave signal for conductivity measurement was very small, which might be affected by the measurement environment. Therefore, the uncertainty of the microwave measurement may contribute to the error bars. It is also noted from Fig. 3 that the deviation of evaluated conductivities from the values tested by the van der Pauw method is 2.03, 7.24, and 11.6% for the Zn, Co, and Al, respectively. One of the causes of this deviation is that the standoff distance variation between different materials may affect the measured voltage, thereby inducing deviation of evaluated conductivity, especially for high-conductivity materials such as Al. Another cause of the deviation may be the evaluation equation which was derived under the plane wave approximation rather than the much more complicated near field analysis. The quantitative evaluation was performed three times, and similar results as shown in Fig. 3 were obtained.

By maintaining a constant standoff distance between the probe tip and sample surface and measuring the microwave signal interaction with the sample, both the topography and electrical properties of the sample were imaged by M-AFM simultaneously. A microwave image of a Au nanowire was successfully created with a resolution on nanometer order. We also demonstrated a novel evaluation equation and calibration technique for the quantitative measurement of the local conductivity. Our results demonstrate that M-AFM can be used to quantitatively measure, *in situ*, the distribution of electrical properties on the nanometer scale.

1) G. Binnig, C. F. Quate, and C. Gerber: Phys. Rev. Lett. **56** (1986) 930.
2) D. Rugar and P. Hansma: Phys. Today **43** [10] (1990) 23.
3) A. Olbrich, B. Ebersberger, and C. Boit: Appl. Phys. Lett. **73** (1998) 3114.
4) J. J. Kopanski, J. F. Marchiando, and J. R. Lowney: J. Vac. Sci. Technol. B **14** (1996) 242.
5) J. E. Stern, B. D. Terris, H. J. Mamin, and D. Rugar: Appl. Phys. Lett. **53** (1988) 2717.
6) M. Nonnenmacher, M. P. O'Boyle, and H. K. Wickramasinghe: Appl. Phys. Lett. **58** (1991) 2921.
7) M. Fujihara and H. Kawate: Thin Solid Films **242** (1994) 163.
8) H. Yokoyama and T. Inoue: Thin Solid Films **242** (1994) 33.
9) Y. Ju, K. Inoue, M. Saka, and H. Abé: Appl. Phys. Lett. **81** (2002) 3585.
10) K. Lai, W. Kundhikanjana, M. Kelly, and Z. X. Shen: Rev. Sci. Instrum. **78** (2007) 063702.
11) A. Karbassi, D. Ruf, A. D. Bettermann, C. A. Paulson, and Daniel W. van der Weide: Rev. Sci. Instrum. **79** (2008) 094706.
12) A. N. Reznik and V. V. Talanov: Rev. Sci. Instrum. **79** (2008) 113708.
13) H. P. Huber, M. Moertelmaier, M. Wallis, C. J. Chiang, and M. Hochleitner: Rev. Sci. Instrum. **81** (2010) 113701.
14) D. E. Steinhauer, C. P. Vlahacos, F. C. Wellstood, S. M. Anlage, C. Canedy, R. Ramesh, A. Stanishevsky, and J. Melngailis: Appl. Phys. Lett. **75** (1999) 3180.
15) X. Y. Zhang, X. C. Wang, F. Xu, Y. G. Ma, and C. K. Ong: Rev. Sci. Instrum. **80** (2009) 114701.
16) F. Duewer, C. Gao, I. Takeuchi, and X. D. Xiang: Appl. Phys. Lett. **74** (1999) 2696.
17) Y. Ju, H. Sato, and H. Soyama: Proc. InterPACK2005, 2005, p. 1919.
18) Y. Ju, T. Kobayashi, and H. Soyama: Microsyst. Technol. **14** (2008) 1021.
19) Y. Ju, M. Hamada, T. Kobayashi, and H. Soyama: Microsyst. Technol. **15** (2009) 1195.
20) L. Zhang, Y. Ju, A. Hosoi, and A. Fujimoto: Rev. Sci. Instrum. **81** (2010) 123708.
21) A. Fujimoto, L. Zhang, A. Hosoi, and Y. Ju: Microsyst. Technol. **17** (2011) 715.
22) Y. Ju, Y. Hirosawa, H. Soyama, and M. Saka: Appl. Phys. Lett. **87** (2005) 162102.
23) D. M. Pozer: *Microwave Engineering* (Wiley, New York, 1998) 2nd ed., p. 32.
24) L. S. Liu and Y. Ju: Rev. Sci. Instrum. **81** (2010) 124701.